



PAPER • OPEN ACCESS

## Fe-doped tricalcium phosphates: crystal structure and degradation behavior

To cite this article: Kyung-Hyeon Yoo *et al* 2020 *Mater. Res. Express* **7** 125403

View the [article online](#) for updates and enhancements.

You may also like

- [Beta-tricalcium phosphate promotes osteogenic differentiation of bone marrow-derived mesenchymal stem cells through macrophages](#)  
Mengting Zheng, Mengjia Weng, Xiaoyu Zhang *et al.*
- [In vivo stability evaluation of Mg substituted low crystallinity  \$\beta\$ -tricalcium phosphate granules fabricated through dissolution–precipitation reaction for bone regeneration](#)  
Garima Tripathi, Yuki Sugiura, Kanji Tsuru *et al.*
- [Bone engineering by phosphorylated-pullulan and -TCP composite](#)  
Tomohiro Takahata, Takumi Okihara, Yasuhiro Yoshida *et al.*

**ECS**  
The  
Electrochemical  
Society  
Advancing solid state &  
electrochemical science & technology

**DISCOVER**  
how sustainability  
intersects with  
electrochemistry & solid  
state science research

# Materials Research Express



## PAPER

# Fe-doped tricalcium phosphates: crystal structure and degradation behavior

### OPEN ACCESS

#### RECEIVED

10 September 2020

#### REVISED

25 November 2020

#### ACCEPTED FOR PUBLICATION

30 November 2020

#### PUBLISHED

16 December 2020

Original content from this work may be used under the terms of the [Creative Commons Attribution 4.0 licence](#).

Any further distribution of this work must maintain attribution to the author(s) and the title of the work, journal citation and DOI.



Kyung-Hyeon Yoo<sup>1</sup> , Hyeonjin Kim<sup>1</sup>, Woo Gyeong Sun<sup>1</sup>, Yong-Il Kim<sup>2</sup> and Seog-Young Yoon<sup>1</sup>

<sup>1</sup> School of Materials Science and Engineering, Pusan National University, Busan, Republic of Korea

<sup>2</sup> Department of Orthodontics, Dental Research Institute, Pusan National University, Yangsan 50612, Republic of Korea

E-mail: [syy3@pusan.ac.kr](mailto:syy3@pusan.ac.kr)

**Keywords:** iron-doped tricalcium phosphate, crystal structure, *in vitro* behavior, degradation, resorption, cell adhesion

Supplementary material for this article is available [online](#)

## Abstract

$\beta$ -tricalcium phosphate ( $\beta$ -TCP,  $\text{Ca}_3(\text{PO}_4)_2$ ) is biodegradable ceramics with chemical and mineral compositions similar to those of bone. It is a potential candidate for bone repair surgery, and substituting the Fe ions can improve its biological behavior. In this study, we investigated the effect of Fe ions on the structural deviation and *in vitro* behavior of  $\beta$ -TCP. Fe-doped  $\beta$ -TCP were synthesized by the co-precipitation method, and the heat treatment temperature was set at 1100 °C. The chemical state of the Fe-doped  $\beta$ -TCP was analyzed by x-ray photoelectron spectroscopy, while structural analysis was carried out by Rietveld refinement using the x-ray diffraction results. Fe ions existed in both  $\text{Fe}^{2+}$  and  $\text{Fe}^{3+}$  states and occupied the Ca-(4) and Ca-(5) sites. Fe ions enhanced the degradation of  $\beta$ -TCP and resorption behavior onto the surface of  $\beta$ -TCP during the immersion test. As a result, Fe ion improves the initial cell adhesion and proliferation behavior of  $\beta$ -TCP.

## 1. Introduction

$\beta$ -tricalcium phosphate ( $\beta$ -TCP,  $\text{Ca}_3(\text{PO}_4)_2$ ) is one of the biocompatible, osteoconductive, and biodegradable calcium phosphate ceramics [1–5]. It is stable at room temperature and transition into  $\alpha$ -TCP above  $1150 \pm 30$  °C [6, 7]. It has been widely used for medical applications such as bone tissue engineering, drug delivery systems [8–10], and bone reconstruction [11–13]. However,  $\beta$ -TCP has a lack of osteoinductive properties [2]. Ion substitution is known as an effective way to modify the osteoinduction of  $\beta$ -TCP. Especially, essential trace elements for proper functioning of the human body such as Mg [14–16], Zn [17, 18], Sr [19, 20], Na [21, 22], K [21, 22], etc [23, 24] are used for  $\text{Ca}^{2+}$  ion substitution. These essential trace elements influence the bone formation process by themselves [25, 26] and affect the structural and chemical properties of  $\beta$ -TCP [14–24].

Among the trace elements, Fe, which exists in blood and bone marrow, plays an essential role in the human body involving vitamin D metabolism and maturation of collagen [26–30]. Also, iron promotes the nucleation of apatites [31] and has a hyperthermia effect required for cancer therapy [32]. Therefore, various studies have shown that Fe ions affect the crystallinity, solubility [33–35], and bioactivity of calcium phosphate [36–38]. Especially for  $\beta$ -TCP, Guangda Li *et al* reported that Fe-doped  $\beta$ -TCP shows antibacterial properties [38]. Although various studies have been carried out to investigate the effect of Fe ions on the properties of  $\beta$ -TCP [39, 40], the effect of Fe-doping on the degradation behavior for  $\beta$ -TCP has not been investigated yet.

The structure change occurring when Fe ions are substituted to  $\beta$ -TCP affects its physicochemical properties, especially degradation behavior. Since Fe ions (both  $\text{Fe}^{2+}$  and  $\text{Fe}^{3+}$ ) are smaller than the  $\text{Ca}^{2+}$  ion and have different charge valences (in the case of  $\text{Fe}^{3+}$ ), Fe substitution changes the interatomic distance and lattice constants of  $\beta$ -TCP [40, 41]. Previous studies have shown that the Fe substitution-induced structural changes of  $\beta$ -TCP depend on the amount of Fe ions [38].

In this study, the structure and chemical states of Fe-doped  $\beta$ -TCP calcined at 1100 °C were studied in detail. To investigate the structural changes, various Fe-doped  $\beta$ -TCP powder was synthesized with different amounts of Fe ion concentration. Structural analysis was carried out using Rietveld refinement. Also, the effect of the Fe

ion on the  $\beta$ -TCP on its degradation behavior was studied through immersion in the culture medium. After the immersion test, the effect of the degraded material and by-product on cell behavior were also evaluated. Fe contained tricalcium phosphate could be used for various biomedical applications such as bone graft [42, 43], drug delivery systems [44, 45], and dental implants [46]. Also, It is expected that it will be more utilize variously through surface coating [42, 46].

## 2. Experimental procedure

### 2.1. Preparation of Fe-doped $\beta$ -TCP powder

$\beta$ -TCP and Fe-doped  $\beta$ -TCP were prepared by the co-precipitation method.  $\text{Ca}(\text{NO}_3)_2 \cdot 4\text{H}_2\text{O}$  (Junsei, >98%),  $(\text{NH}_4)_2\text{HPO}_4$  (Junsei, >99%), and  $\text{Fe}(\text{NO}_3)_3 \cdot 9\text{H}_2\text{O}$  (Junsei, >99%) were used as the Ca, P, Fe ions precursors, respectively. To prepare pure  $\beta$ -TCP powder,  $\text{Ca}(\text{NO}_3)_2 \cdot 4\text{H}_2\text{O}$  and  $(\text{NH}_4)_2\text{HPO}_4$  were dissolved in deionized (DI) water under stirring at 45 °C for 30 min  $\text{Ca}(\text{NO}_3)_2 \cdot 4\text{H}_2\text{O}$  was added dropwise ( $13 \text{ ml min}^{-1}$ ) to  $(\text{NH}_4)_2\text{HPO}_4$ . To synthesize the Fe-doped  $\beta$ -TCP powder, various Fe ion concentrations (3, 6, 9 mol%) were used while maintaining a (Ca+Fe)/P ratio of 1.5.  $\text{Ca}(\text{NO}_3)_2 \cdot 4\text{H}_2\text{O}$  and  $\text{Fe}(\text{NO}_3)_3 \cdot 9\text{H}_2\text{O}$  were dissolved in DI water (solution 1), and  $(\text{NH}_4)_2\text{HPO}_4$  was dissolved separately in DI water (solution 2). Solution 2 was stirred at 45 °C for 30 min, and solution 1 was slowly added dropwise ( $13 \text{ ml min}^{-1}$ ) to it. The pH of the resulting solutions was maintained at 7 by adding  $\text{NH}_4\text{OH}$ . The solution was stirred for 2 h at 45 °C (500 rpm), and aged 1 day at a water bath (40 °C) for the precipitate maturation. The precipitated suspension was washed and filtered to remove unreacted products with 1 l of D.I. water. After filtration, dried at 80 °C for one day and ground into fine powders. The four samples were labeled as Fe 0, Fe 1, Fe 2, and Fe 3. After the drying process, each powder was calcined at 1100 °C for 2 h (at a heating rate of 6 °C  $\text{min}^{-1}$  and natural cooling) in the air.

### 2.2. Powder characterization

To analyze the thermal stability, each 10 mg of dried powders were subjected to differential scanning calorimeter (DSC, STA 8000, PerkinElmer Inc., Ma, USA) using a heating rate of 25 °C  $\text{min}^{-1}$  and a peak temperature of 1400 °C in an oxygen atmosphere (for a flow rate of 20  $\text{ml min}^{-1}$ ). X-ray diffraction patterns (XRD, Ultima 4, Rigaku Corp., Japan) were obtained to identify the phase of the calcined powder using  $\text{Cu K}\alpha$  radiation (1.540562 Å). The diffractometer operated at 40 kV, 40 mA, and a step size of 0.01, and counting of 8 s were used. To obtain the crystallographic information file (CIFs) for the synthesized samples, we used an integrated x-ray powder diffraction software package PDXL (Rigaku, Version 2.1.3.4) ICSD card no. 97500. The structural analysis revealed that the  $\beta$ -TCP powder showed an R3c space group. The crystal structure analysis of the calcined powder was carried out by Rietveld refinement using Fullprof software. The global instability (GII) was also calculated by the BondStr program in Fullprof.

X-ray photoelectron spectroscopy (Theta Probe AR-XPS, Thermo Fisher Scientific, Waltham, MA, USA) was performed using a theta probe AR-XPS using a monochromatic Al  $\text{K}\alpha$  (1486.6 eV) at 15 kV and 150 W. The composition of the samples was observed using an inductively coupled plasma atomic emission spectrophotometer (ICP-AES, ACTIVA, JY HORIBA), 0.05 g of samples were pretreated with 2 ml of nitric acid and 1 ml of hydrochloric acid solution.

### 2.3. Degradation test

For the degradation test, cylindrical samples ( $D = 10 \text{ mm}$  and  $H = 2 \text{ mm}$ ) were prepared by the press (2 tons for 5 min) and sintered at 1100 °C for 10 h (at a heating rate of 6 °C  $\text{min}^{-1}$  and natural cooling). For degradation test with culture medium, full media containing minimal essential medium-alpha ( $\alpha$ -MEM, Gibco), 10% fetal bovine serum (FBS, Merck), 1% penicillin-streptomycin (PS, Gibco), and 5  $\mu\text{g ml}^{-1}$  plasmocin (InvivoGen, San Diego, CA) was prepared. The cylindrical samples were immersed in a culture medium (pH 7.71) for 1 day and 5 days (37 °C, 50 rpm), respectively. After the degradation test, the mass loss (%) of samples measured after washing (D.I. water) and drying (37 °C).

$$\text{Mass loss(\%)} = (W_i - W_d) / W_i \times 100 (W_i: \text{initial weight}, W_d: \text{weight after degradation})$$

$$\text{Mass loss(\%)} = \frac{(W_i - W_d)}{W_i} \times 100$$

( $W_i$ : initial weight,  $W_d$ : weight after degradation)

### 2.4. Cell behavior related to degradation

To evaluate the effect of degradation on cell behavior, cell proliferation, and adhesion tests were performed by Cholecystokinin octapeptide assay (CCK-8) and field emission scanning electron microscopy (SEM, MIRA3, TESCAN) images. For cell tests, the hDPSCs at passage 7 were used. Cell proliferation was assessed using

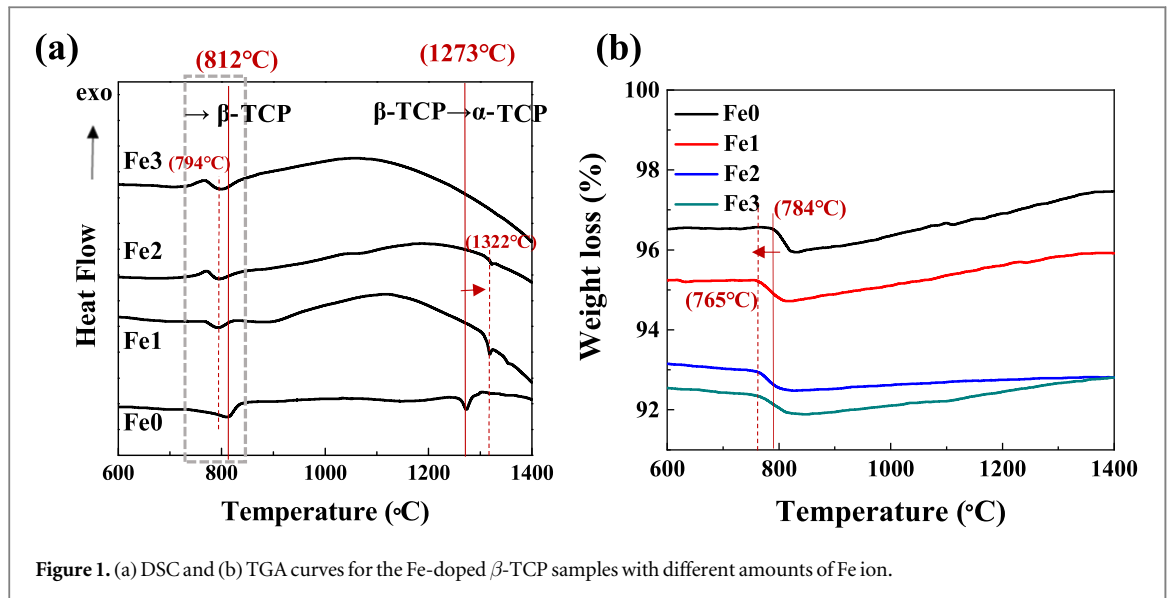


Figure 1. (a) DSC and (b) TGA curves for the Fe-doped  $\beta$ -TCP samples with different amounts of Fe ion.

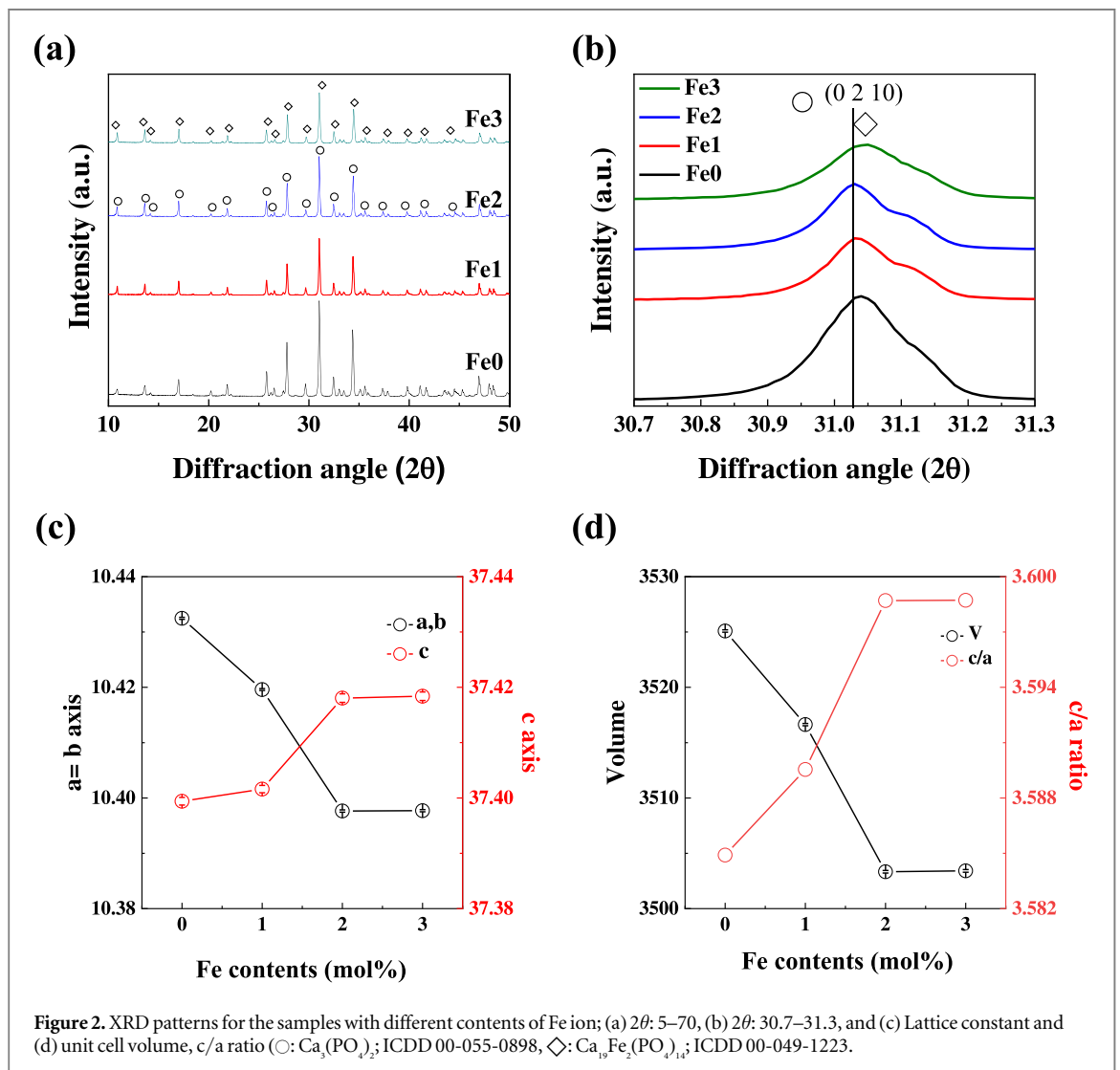


Figure 2. XRD patterns for the samples with different contents of Fe ion; (a)  $2\theta$ : 5–70, (b)  $2\theta$ : 30.7–31.3, and (c) Lattice constant and (d) unit cell volume, c/a ratio ( $\circ$ :  $\text{Ca}_3(\text{PO}_4)_2$ ; ICDD 00-055-0898,  $\diamond$ :  $\text{Ca}_{19}\text{Fe}_2(\text{PO}_4)_{14}$ ; ICDD 00-049-1223).

D-Plus™ CCK cell viability assay kit (Donginbio, KOREA). The hDPSCs were cultured  $1 \times 10^4$  cells in 48-well plates and incubated for 1 day before treatment. After 1 day, the culture medium was replaced with extracted culture medium (after degradation test day1, day5) and incubated for 1, 2, 3 days. Subsequently, cells were

**Table 1.** Notation of different amounts of Fe ions substituted in  $\beta$ -TCP samples.

Sample notation	Fe mol% (calculated)	Fe mol% (measured by ICP-AES)
Fe0	0	0
Fe1	3	2.82
Fe2	6	5.78
Fe3	9	8.83

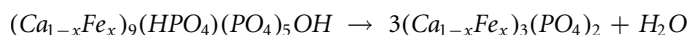
treated with 20  $\mu$ l CCK per well and incubated for 1 h at 37 °C. The absorbance of the resulting solution was measured by a plate reader at 450 nm.

To evaluate the cell adhesion behavior, the morphology of adhered on the sample surface was investigated. After immersed in culture medium for 1, 5 days,  $1 \times 10^5$  cells were seeded on the cylindrical sample (for control, using non-degraded sample) for 1 day. All samples were washed in phosphate buffer saline (PBS) and fixed in 4% paraformaldehyde (PFA)/2.5% glutaraldehyde in PBS for 30 min. Afterward, the samples were washed with D.I. water and dehydrated (30, 50, 70, 90, 94, 100 vol% ethanol, each for 15 min). Drying the samples were using ethanol-hexamethyldisilazane (HMDS, Sigmaaldrich) solution at a 50, 100 vol% of HMDS (each 15 min at RT). After drying, all samples were coated with gold and observed by FE-SEM (at 5 kV).

### 3. Results and discussion

#### 3.1. Powder characterization

The effect of Fe substitution on the phase transition temperature of the  $\beta$ -TCP samples was investigated with their DSC and TGA curves (figure 1). It shows an endothermic peak around 740 °C – 840 °C (figure 1(a)). This endothermic peak is associated with the dehydroxylation of the amorphous apatite (CDHA) phase into  $\beta$ -TCP [46]. It might be attributed to removing the OH ions of CDHA, as reported in the following chemical reaction [47]:



For Fe-doped samples (Fe1, Fe 2, and Fe 3), the endothermic peak in DSC curves was shifted to lower temperatures (figure 1(a)). Also, in the presence of Fe ions (Fe 1, Fe 2, and Fe 3), characteristic peaks of exothermic reactions were observed before the formation of  $\beta$ -TCP (around 740 °C). These peaks would be related to Fe and P ions because it is similar to the exothermic behavior when water molecules were lost in  $FePO_4 \cdot 2H_2O$  [48]. According to previous results related to Mg-doped TCP [49], these exothermic peak related dehydroxylation reaction. Around 1260 °C, except for the Fe3 sample, all the samples showed peaks corresponding to the  $\beta \rightarrow \alpha$  phase transition [14, 48, 50]. This result revealed that the Fe3 sample had a different thermal behavior compared to  $\beta$ -TCP. This behavior will be explained with the XRD pattern later. In addition, the phase transition ( $\beta \rightarrow \alpha$ ) temperature increased with increasing the amount of Fe ions, suggesting that Fe ion improves the thermal stability of the  $\beta$ -TCP phase [48]. Compared to Mg-doped TCP, Fe-doped TCP is more stable (Mg 1%: 1270, Mg 3%: 1330 °C) [48, 50]. TGA curves of Fe-doped TCP powder showed weight losses (figure 1(b)). The weight loss that occurred between 760 °C, and 820 °C was attributed to the loss of water, and this reaction is related to the formation of  $\beta$ -TCP [50]. The ICP results of the samples (Table. 1) revealed that  $\beta$ -TCP consisted of Fe ions.

The XRD patterns of the Fe-doped  $\beta$ -TCP powder calcined at 1100 °C are shown in figures 2(a) and (b). All the samples (except for Fe3) showed only the single phase of  $\beta$ -TCP (ICDD 00-055-0898), and these results are consistent with those reported previously (no secondary phase was formed when <7.5 mol% of Fe ions were present) [40, 41]. On the point of the main peak (figure 2(b)), the peak moved to the left as the amount of Fe ions increased. These phenomena can explain with the variation of lattice parameter with the substitution of Fe ion in  $\beta$ -TCP. In figures 2(c) and (d) show the changes in the lattice constants and volume of the samples as a function of the amount of Fe ions. The lengths of the a, b axes decreased with an increase in the amount of Fe because the radius of  $Fe^{2+}$  (0.78 Å) and  $Fe^{3+}$  (0.64 Å) ions was smaller than  $Ca^{2+}$  (0.99 Å) ion. Therefore, the presence of Fe ions reduced the unit cell volume of  $\beta$ -TCP, and it increases the thermal stability of  $\beta$ -TCP [46]. On the other hand, the main peak for the Fe3 sample moved to the right (as shown in figure 2(b)) compared to Fe1 and Fe2 samples. It would be attributed to the formation of the  $Ca_{19}Fe_2(PO_4)_{14}$  (ICDD 00-049-1223) phase as a secondary phase due to the excess addition of Fe ions [38]. Fe ions contained calcium phosphate, as for the calcium iron phosphate ( $Ca_9Fe(PO_4)_7$ ), it has no phase transition between room temperature and 1400 °C [47].

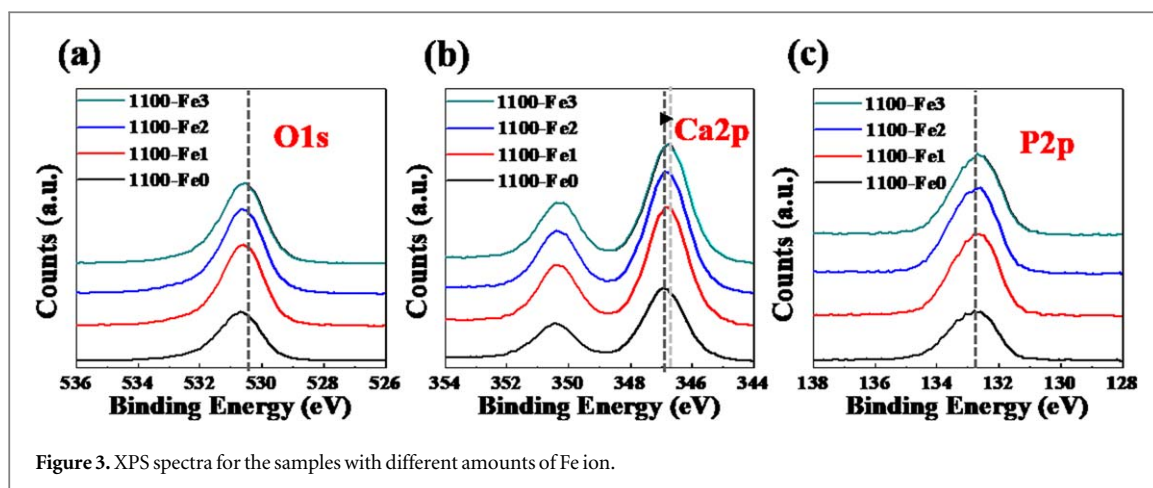


Figure 3. XPS spectra for the samples with different amounts of Fe ion.

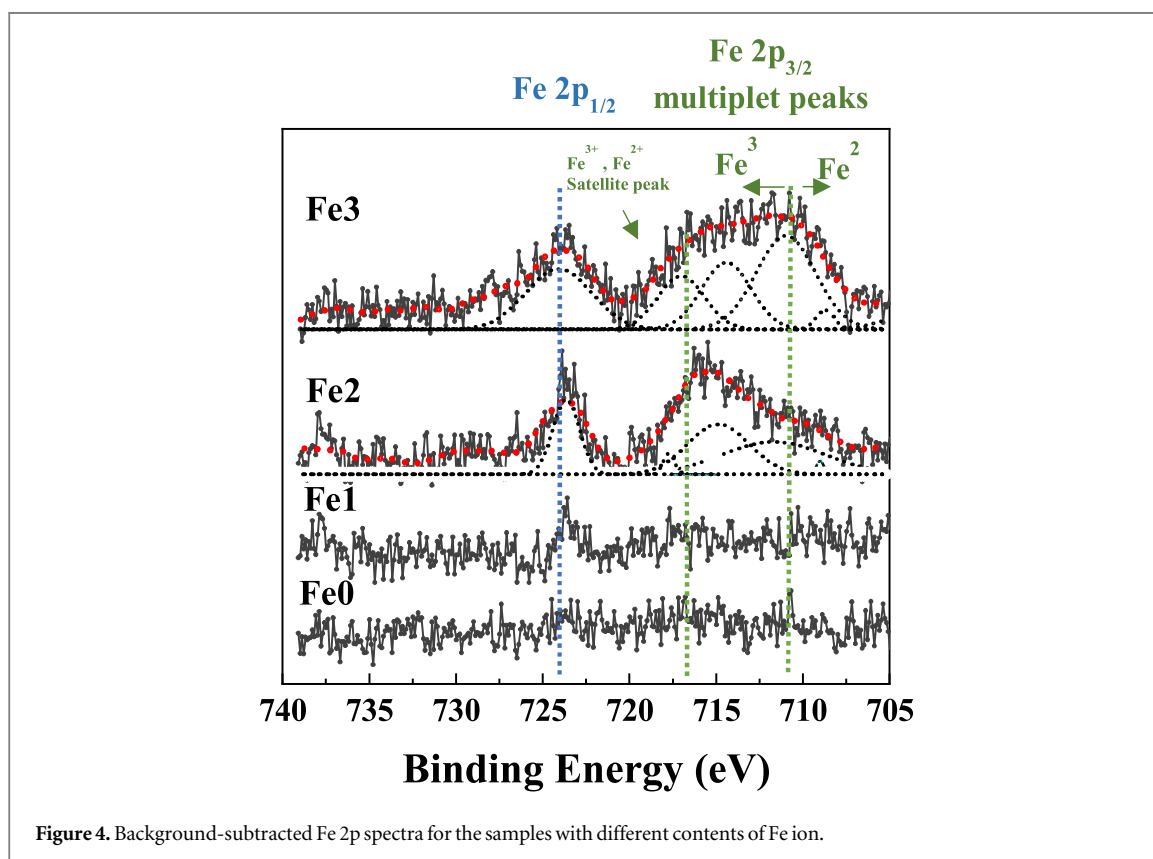


Figure 4. Background-subtracted Fe 2p spectra for the samples with different contents of Fe ion.

Therefore, it would explain why secondary phase has no endothermic peak corresponding to the phase transition ( $\beta \rightarrow \alpha$ ) as shown in the DSC result in figure 1.

### 3.2. Substitution states and site of Fe-doped $\beta$ -TCP

The high-resolution XPS spectra of the Fe-doped  $\beta$ -TCP samples with different Fe ion contents (0, 3, 6, and 9 mol%) are shown in figures 3 and 4. Figure 3 shows the O 1s, Ca 2p, P 2p spectra [6, 51, 52], and the peak positions are summarized in table 2. It can be seen that the Ca 2p peak at 346.9 eV of the Fe 0 sample decreased in comparison with that of the Ca 2p peak in Fe3 peak (346.77 eV). This shifting of binding energy can be ascribed to the interaction between  $\text{Ca}^{2+}$  and  $\text{Fe}^{2+}$  or  $\text{Fe}^{3+}$  ions. The Fe 2p spectra (Fe 2p<sub>3/2</sub> and Fe 2p<sub>1/2</sub> peaks, 740–700 eV) of the samples are shown in figure 4. These Fe 2p peaks can be attributed to  $\text{Fe}_3\text{O}_4$  [52–55], and the multiple peaks that come from binding energies higher than 710 eV can be corresponded to  $\text{Fe}^{3+}$  ions. On the other hand, peaks that occurred at lower than 710 eV can be attributed to  $\text{Fe}^{2+}$  ions [52, 53].

In general, the  $\beta$ -TCP supplies different substitution sites depending on the types of substituting metal ions [21, 56]. Figure 5 shows the schematic diagram for the available substitution site while replacing the Fe ion with Ca ion in the  $\beta$ -TCP phase. As shown in figure 5, Fe ions can coexist as divalent ion and trivalent ion. Therefore,

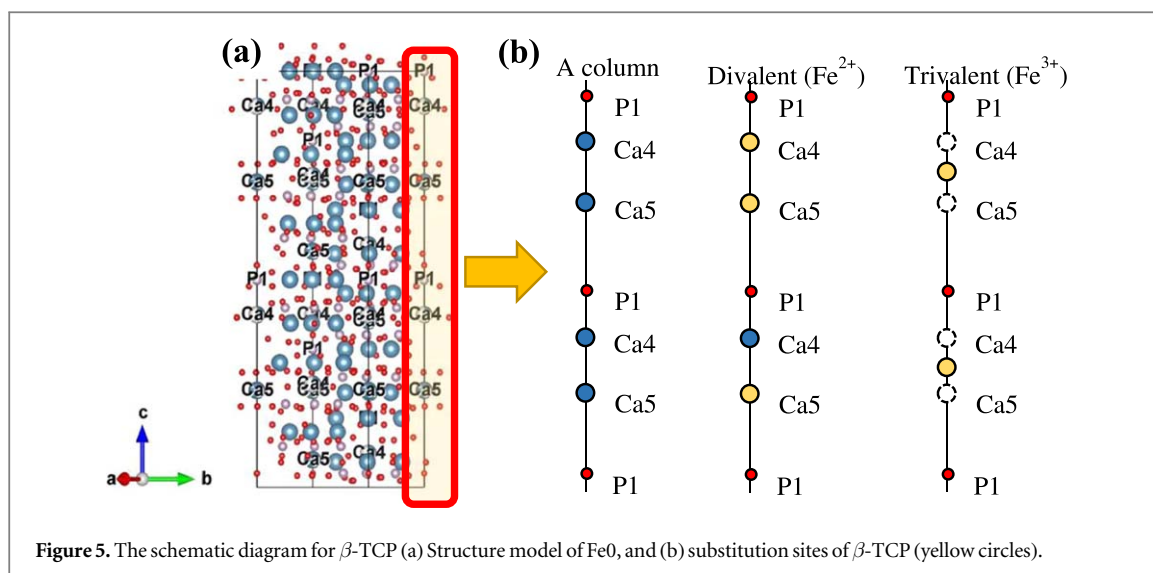


**Table 2.** Binding energies and atomic ratios on the surface of samples.

Sample notation	Peak position (eV)			Atomic ratio (Ca+Fe)/P	
	O 1s	Ca 2p <sub>2/3</sub>	P 2p	Surface (XPS)	Measured (ICP)
Fe0	530.69	346.9	132.79	1.35	1.50
Fe1	530.6	346.8	132.7	1.30	1.47
Fe2	530.61	346.81	132.76	1.28	1.47
Fe3	530.59	346.77	132.68	1.35	1.48

**Table 3.** Rietveld refinement results for the Fe-doped  $\beta$ -TCP samples. Reliability factors, site occupancy, and inter-atomic distance of the substitution sites.

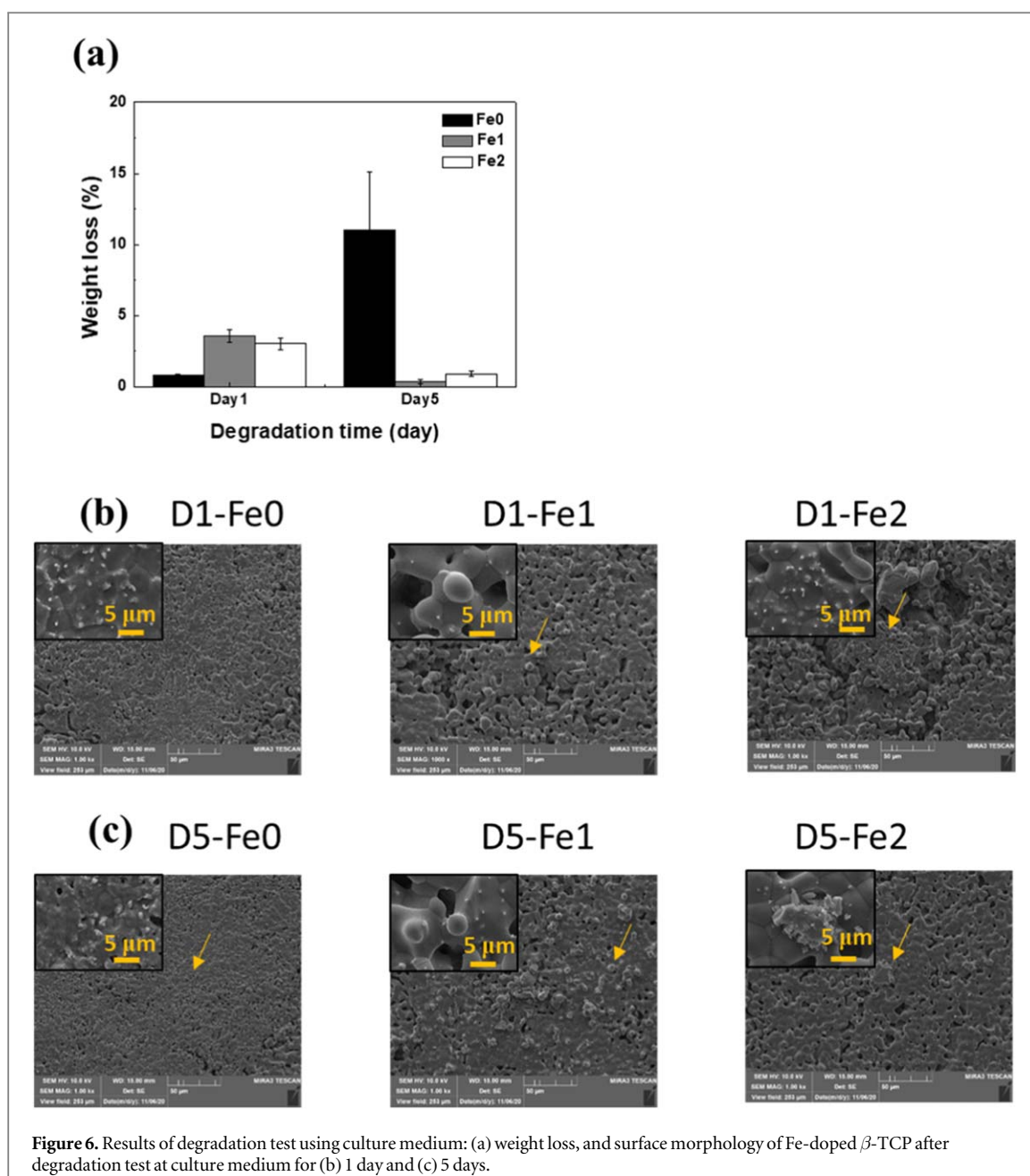
Sample	Reliability factors (%) R <sub>p</sub> /R <sub>wp</sub> /R <sub>exp</sub> /R <sub>Bragg</sub>	Ca(5) site Occ.		Ca(4) site Occ.			Ca(4)—P(1)	GII
		Ca	Fe	Ca	Fe	sum		
Fe0	6.17/8.58/4.45/3.01	0.99	0.0	0.429	0.0	0.429	3.0(11)	0.56
Fe1	6.73/9.83/6.10/2.94	0.82	0.18	0.38	0.071	0.451	3.0(11)	0.64
Fe2	6.51/9.15/6.1/2.28	0.62	0.38	0.21	0.12	0.33	3.3(11)	0.68
Fe3	6.59/9.24/6.1/2.47	0.43	0.57	0.26	0.06	0.32	3.4(16)	0.60

Ca-(4) and Ca-(5) sites are considered an alternative to substitution sites. Previous studies have shown that Fe<sup>3+</sup> ions substituted in Ca-(5) sites and simultaneously vacancies are formed in Ca-(4) sites, resulting in decreasing the site occupancy for Ca-(4) sites [21, 56]. In the case of Fe<sup>2+</sup> ions, it can substitute both Ca-(5) sites and vacancy of Ca-(4) sites. Therefore, when Fe<sup>2+</sup> ions are substituted to TCP structure, the site occupancy for Ca-(4) sites increase [21, 56].

To identify the site occupancy for substitution Fe ion in Ca site in  $\beta$ -TCP, the Rietveld refinement was carried out. The results were summarized in table 3 and figure S1 (available online at [stacks.iop.org/MRX/7/125403/mmedia](https://stacks.iop.org/MRX/7/125403/mmedia)). As can be seen in table 3, the site occupancy of Fe ions and the distance between Ca-(4) and P-(1) sites were increased with increasing the amount of substituted Fe ions. The total occupancy at the Ca-(4) sites increased with increasing of the content of Fe ions because Fe ions are substituted at Ca-(4), vacancy at Ca-(4), and Ca-(5) sites. Also, the substitution of Fe ions (which are smaller than Ca ions) into Ca-(4) sites increases the distance between the Ca-(4) and the surrounding cations(P-(1)) due to the repulsive force between them [53]. In the point of GII (global instability index), the value of GII was increased with an increase in the content of Fe ion. It implies that the crystallinity of Fe-doped  $\beta$ -TCP was more unstable with the addition of Fe ion, which will accelerate the degradation behavior [57].

### 3.3. In vitro degradation behavior of Fe-doped $\beta$ -TCP

The results of immersion in the culture medium during 1 and 5 days are shown in figure 6. As shown in figure 6(a), the weight loss of the Fe 0 sample was lower than the Fe 1 and Fe 2 samples after 1 day. However, after



5 days of Fe 0 sample, the weight loss was higher than the others. It implies that the Fe ion increases the  $\beta$ -TCP degradation rate and resorption of calcium phosphates onto the surface of  $\beta$ -TCP during in vitro experiments [58]. As can be seen in figures 6(b), (c), and S2, the new by-products (arrow) were observed on the surface. These by-products were analyzed by EDS point mapping (figure S2). In figure S2, the small particle named A is composed of Ca, P, Si ions. In the case of Fe1, Fe2 samples, large adsorbate is also observed on the surface, which is considered to be a calcium phosphate material because it is composed of Ca and P. As a result, the substitution of Fe ion in  $\beta$ -TCP can enhance the degradation behavior and the formation of new calcium phosphates. According to previous research [59], adsorption occurs well in grains in the c-axis because of local residual charge. Therefore, new calcium phosphate by-products were more adsorbed in Fe-doped samples, which have a longer length of c-axis.

### 3.4. Cell morphology with immersion time

To observe the variation of cell morphology, the cell adhesion test was carried out with a cell culture medium for 1 day. After the cell adhesion test, the microstructure of the surface was observed with the aid of SEM. As shown in figure 7, the new calcium phosphates on the surface of each sample were formed (represent by arrow). The cells seeded on the surfaces displayed elongated, branched shapes and formed clusters (dash). As shown in figure 7(a) (without immersion time), the Fe 1 and Fe 2 samples had more cell populations compared to Fe 0

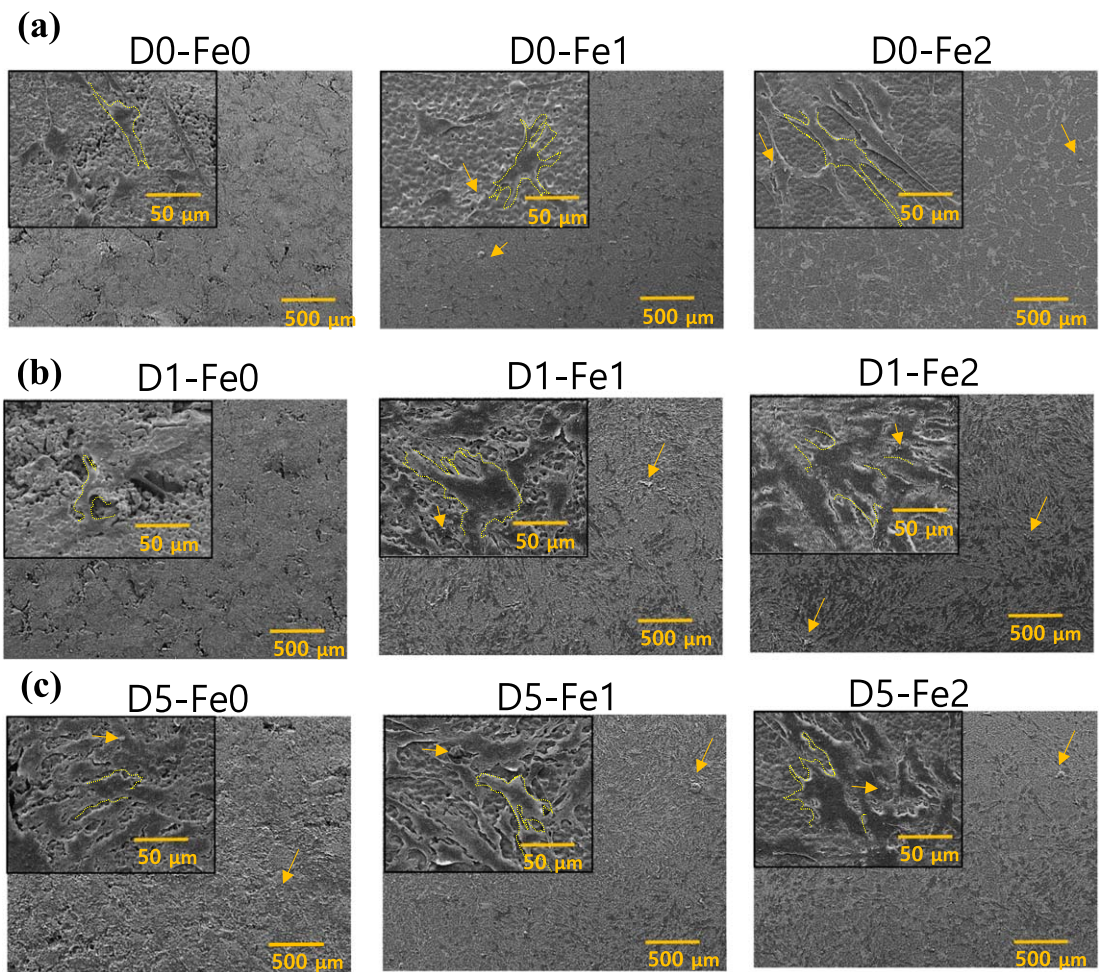


**Figure 7.** The morphology of hDPSC on the Fe-doped  $\beta$ -TCP disc (1 day cultured): (a) non-immersed disc (D0) and after degradation test (b) 1 day (D1) (c) 5 days (D5).

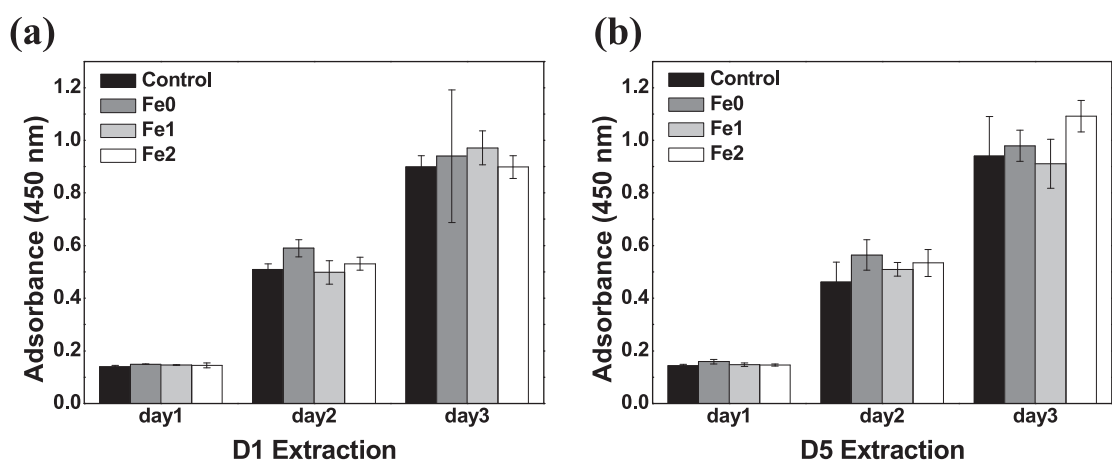


**Figure 8.** The proliferation of hDPSC with degraded by-product: Extracted culture medium for (a) 1 day and (b) 5 days (control: culture medium stored at 37 °C for 1, 5 days).

sample, indicating the Fe ions help the cell attachment onto the surface of the  $\beta$ -TCP sample. Besides, the cell adhesion behavior was improved with Fe ion.

As shown in figures 7(b) and (c), the cell attachment was more plentiful than compared to without pre-immersed in culture medium (figure 7(a)). There were increases in cell coverage onto the surface with increasing of the immersion time (0 to 5 days) except for the Fe 0 sample. It suggests that the cell adhesion could extensively spread out the surface when the resorption of new calcium phosphates onto the sample surface proceed. The

resorption process can be observed on Fe-doped samples after immersion test following the degradation process. In the case of the Fe 0 sample, cell adhesion did not proceed significantly at D 0 and D 1-Fe 0 samples because the Fe 0 sample was only degraded until 5 days without the resorption process as shown in figure 6(a). Therefore, the Fe ion enhanced the degradation behavior of  $\beta$ -TCP and helped the formation of new calcium phosphate onto the surface of  $\beta$ -TCP during the immersion test. These results induced that the doped Fe ions can improve the initial cell adhesion and proliferation behavior.

### 3.5. Effects of degradation by-products on cell proliferation

From the results of the previous degradation test, it was confirmed that resorption occurred on the 5 days (in figure 6). Also, the results of the cell adsorption experiment confirmed that cell adhesion occurs more easily in Fe ion-doped TCP (in figure 7). Finally, a cell proliferation test was performed to confirm the cell proliferation of the by-products in which decomposition and resorption occurred. Figure 8 presents the results of cell proliferation using extracted culture medium after samples immersed for 1, 5 days. Absorbance values increased for 3 days in all specimens and were higher than the control. Also, the degradation by-products for Fe 2 samples showed the highest cell proliferation. These results found that the Fe 0, Fe 1, and Fe 2 samples did not show any cytotoxicity against hDPSC, indicating good biocompatibility. This also suggests that all samples may have better physiological compatibility.

When calcium phosphate is degraded, and ion elution occurs, cell proliferation should be better [60, 61]. However, there was no significant difference in comparing cell proliferation using a solution extracted after 1 day and 5 days. There would be no significant change in each extract's composition because it was inferred that degradation and resorption simultaneously occurred on the 1 and 5 days.

## 4. Conclusions

The aim of this study was to investigate the effect of Fe substitution on the structure and physicochemical properties of  $\beta$ -TCP. The addition of Fe ion in  $\beta$ -TCP was changed in the range of 3 mol%, 6 mol%, and 9 mol%. Up to 6 mol%, there is no found secondary phase. However, at a 9 mol% content, the  $\text{Ca}_{19}\text{Fe}_2(\text{PO}_4)_{14}$  as the secondary phase was formed. DSC results represent that Fe ions increased the phase transition ( $\beta \rightarrow \alpha$ ) temperature of  $\beta$ -TCP and improved the thermal stability of the  $\beta$ -TCP phase. Because Fe ion is smaller than Ca ion, the lattice volume of Fe-doped TCP is more diminutive than pure TCP. However, the length of the *c*-axis increased because Fe ion substituted in both Ca-(4), a vacancy of Ca-(4), and Ca-(5) sites of  $\beta$ -TCP. In point of *in vitro* behavior, the Fe ion increases the  $\beta$ -TCP degradation rate and resorption of calcium phosphates onto the surface of  $\beta$ -TCP during *in vitro* experiment. Besides, the cell adhesion behavior was more improved with Fe ion. Synthetically, the doped Fe ion in  $\beta$ -TCP enhanced the degradation behavior and helped the resorption of new calcium phosphates onto the surface of  $\beta$ -TCP.

## Acknowledgments

This work was supported by the National Research Foundation of Korea(NRF) grant funded by the Korea government(MSIT) (No.2020R1A2C1014586).

## ORCID iDs

Kyung-Hyeon Yoo  <https://orcid.org/0000-0001-5328-2919>

## References

- [1] Dorozhkin S V and Epple M 2002 *Angewandte Chemie International Edition* **41** 3130
- [2] Kasten P, Luginbühl R, Van Griensven M, Barkhausen T, Krettek C, Bohner M and Bosch U 2003 *Biomaterials* **24** 2593
- [3] LeGeros R Z 2002 *A Publication of the Association of Bone and Joint Surgeons* | *CORR* **395** 81
- [4] Jarcho M 1981 *Clinical Orthopaedics and Related Research* **157** 259
- [5] Ohgushi H, Okumura M, Tamai S, Shors E C and Caplan A I 1990 *Journal of Biomedical Materials Research* **24** 1563
- [6] Carrodeguas R G and De Aza S 2011 *Acta Biomaterialia* **7** 3536
- [7] Matsumoto N, Yoshida K, Hashimoto K and Toda Y 2009 *Materials Research Bulletin* **44** 1889
- [8] Szpalski C, Wetterau M, Barr J and Warren S M 2012 *Tissue Engineering Part B: Reviews* **18** 246
- [9] Mastrogiacomo M, Muraglia A, Komlev V, Peyrin F, Rustichelli F, Crovace A and Cancedda R 2005 *Orthodontics & Craniofacial Research* **8** 277
- [10] Bose S and Tarafder S 2012 *Acta Biomaterialia* **8** 1401
- [11] Schmitz J P, Hollinger J O and Milam S B 1999 *Journal of Oral and Maxillofacial Surgery* **57** 1122
- [12] Horch H H, Sader R, Pautke C, Neff A, Deppe H and Kolk A 2006 *International Journal of Oral and Maxillofacial Surgery* **35** 708

- [13] Huang Y, Jin X, Zhang X, Sun H, Tu J, Tang T, Chang J and Dai K 2009 *Biomaterials* **30** 5041
- [14] Enderle R, Götz-Neunhoffer F, Göbbels M, Müller F A and Greil P 2005 *Biomaterials* **26** 3379
- [15] Frasnelli M and Sglavo V M 2016 *Acta Biomaterialia* **33** 283
- [16] Schroeder L W, Dickens B and Brown W E 1977 *Journal of Solid State Chemistry* **22** 253
- [17] Chou J, Hao J, Kuroda S, Bishop D, Ben-Nissan B, Milthorpe B and Otsuka M 2013 *Marine Drugs* **11** 5148
- [18] Bigi A, Foresti E, Gandolfi M, Gazzano M and Roveri N 1997 *Journal of Inorganic Biochemistry* **66** 259
- [19] Marques C F, Lemos A, Vieira S I, Silva O D C, Bettencourt A and Ferreira J M F 2016 *Ceramics International* **42** 2706
- [20] Ke D, Dernel W, Bandyopadhyay A and Bose S 2015 *Journal of Biomedical Materials Research Part B: Applied Biomaterials* **103** 1549
- [21] Yoshida K, Hyuga H, Kondo N, Kita H, Sasaki M, Mitamura M, Hashimoto K and Toda Y 2006 *Journal of the American Ceramic Society* **89** 688
- [22] Boanini E, Gazzano M and Bigi A 2010 *Acta Biomaterialia* **6** 1882
- [23] Matsumoto N, Sato K, Yoshida K, Hashimoto K and Toda Y 2009 *Acta Biomaterialia* **5** 3157
- [24] Deng Y, Jiang C, Li C, Li T, Peng M, Wang J and Dai K 2017 *Scientific Reports* **7** 1
- [25] Sainz M A, Pena P, Serena S and Caballero A 2010 *Acta Biomaterialia* **6** 2797
- [26] Mertz W 1981 *Science* **213** 1332
- [27] Wada O 2004 *Journal of Japan Medical Association* **47** 351
- [28] Aggett P J 1985 *Clinics in Endocrinology and Metabolism* **14** 513
- [29] Waseem A and Arshad J 2016 *Chemosphere* **163** 153
- [30] Bhattacharya P T, Misra S R and Hussain M 2016 *Scientifica* **2016** 5464373
- [31] Cacciotti I 2016 *Handbook of Bioceramics and Biocomposites* (United Kingdom: Springer) 145978-3-319-12460-5
- [32] Panseri S, Cunha C, D'Alessandro T, Sandri M, Giavaresi G, Marcacci M, Hung C T and Tampieri A 2012 *Journal of Nanobiotechnology* **10** 1
- [33] Pon-On W, Charoenphandhu N, Teerapornpuntakit J, Thongbunchoo J, Krishnamra N and Tang I M 2013 *Materials Chemistry and Physics* **141** 850
- [34] Kaygili O, Dorozhkin S V, Ates T, Al-Ghamdi A A and Yakuphanoglu F 2014 *Ceramics International* **40** 9395
- [35] Morrissey R, Rodriguez-Lorenzo L M and Gross K A 2005 *Journal of Materials Science: Materials in Medicine* **16** 387
- [36] Tampieri A et al 2012 *Acta Biomaterialia* **8** 843
- [37] Nakahira A, Nakamura S and Horimoto M 2007 *IEEE Transactions on Magnetics* **43** 2465
- [38] Li G, Zhang N, Zhao S, Zhang K, Li X, Jing A, Liu X and Zhang T 2018 *Materials Letters* **215** 27
- [39] Singh R K, Srivastava M, Prasad N K, Awasthi S, Dhayan A and Kannan S 2017 *Materials Science and Engineering: C* **78** 715
- [40] Vahabzadeh S, Bose S and Susmita 2017 *Annals of Biomedical Engineering* **45** 819
- [41] Benarafa A, Kacimi M, Gharbage S, Millet J M M and Ziyad M 2000 *Materials Research Bulletin* **35** 2047
- [42] Antoniac I V et al 2020 *Advanced Materials Interfaces* **7** 2000531
- [43] Marc B, Bastien S and Nicola D 2020 *Acta Biomaterialia* **113** 23
- [44] Paul W and Sharma C P 2003 *Journal of Biomaterials Applications* **17** 253
- [45] Sareethammanuwat M, Boonyeun S and Arpornmaeklong P 2020 *Journal of Biomedical Materials Research Part A* **2020** 1-13
- [46] Rau J V, Cacciotti I, Bonis A D, Fosca M, Komlev V S, Latini A, Santagata A and Teghil R 2014 *Applied Surface Science* **307** 301
- [47] Lazoryak B I, Morozov V A, Belik A A, Khasanov S S and Shekhtman V S 1996 Crystal structures and characterization of Ca<sub>9</sub>Fe (PO<sub>4</sub>)<sub>7</sub> and Ca<sub>9</sub>FeH<sub>0.9</sub> (PO<sub>4</sub>)<sub>7</sub> *Journal of Solid State Chemistry* **122** 15
- [48] Marchi J, Dantas A C S, Greil P, Bressiani J C, Bressiani A H A and Müller F A 2007 *Materials Research Bulletin* **42** 1040
- [49] Zhao P, Liu H, Zheng H, Tang Q and Guo Y 2014 *Materials Letters* **123** 128
- [50] Cacciotti I and Bianco A 2011 *Ceramics International* **37** 127
- [51] Lu H B, Campbell C T, Graham D J and Ratner B D 2000 *Analytical Chemistry* **72** 2886
- [52] Mercado D F, Magnacca G, Malandrino M, Rubert A, Montoneri E, Celi L, Bianco Prevot A and Gonzalez M C 2014 *ACS Applied Materials & Interfaces* **6** 3937
- [53] Descostes M, Mercier F, Thromat N, Beaucaire C and Gautier-Soyer M 2000 *Applied Surface Science* **165** 288
- [54] Yamashita T and Hayes P 2008 *Applied Surface Science* **254** 2441
- [55] Dong F, Wang H, Wu Z and Qiu J 2010 *Journal of Colloid and Interface Science* **343** 200
- [56] Yashima M, Sakai A, Kamiyama T and Hoshikawa A 2003 *Journal of Solid State Chemistry* **175** 272
- [57] Gallo M et al 2019 *Acta Biomaterialia* **89** 391
- [58] Gallo M, Tadier S, Meille S and Chevalier J 2018 *Journal of the European Ceramic Society* **38** 899
- [59] Tao J, Jiang W, Zhai H, Pan H, Xu X and Tang R 2008 *Crystal Growth and Design* **8** 2227
- [60] Barrère F, van Blitterswijk C A and de Groot K 2006 *International Journal of Nanomedicine* **1** 317
- [61] Schaefer S, Detsch R, Uhl F, Deisinger U and Ziegler G 2011 *Advanced Engineering Materials* **13** 342